

Supporting Information

Mechanism of Regulation of Expression of the β -Lactam Antibiotic-Resistance Determinants in Methicillin-Resistant *Staphylococcus aureus* (MRSA)

Blas Blázquez[§], Leticia I. Llarrull[†], Juan R. Luque-Ortega[‡], Carlos Alfonso[‡], Bill Boggess[§] and Shahriar Mobashery^{§*}

[§]Department of Chemistry and Biochemistry, University of Notre Dame, Notre Dame 46556, IN, USA

[†]Institute of Molecular and Cell Biology of Rosario (IBR), CONICET-UNR; Department of Biological Chemistry, Biophysics Area, National University of Rosario (UNR), Rosario, 2000, Argentina

[‡]Centro de Investigaciones Biológicas - CSIC, Ramiro de Maeztu 9, Madrid 28040, Spain

Contents

Experimental Procedures	SI2
Figure S1. SDS-PAGE analysis of the purified MecI	SI3
Figure S2. MALDI mass spectrum of MecI	SI4
Figure S3. SDS-PAGE analysis of the purified BlaI	SI4
Figure S4. EMSA showing the binding of MecI	SI5
Figure S5. EMSA showing the binding of BlaI	SI5
Figure S6. Sedimentation velocity assay	SI6
Figure S7. Sedimentation equilibrium of MecI	SI7
Figure S8. Oligomerization state of MecI protein in solution	SI7
Figure S9. MecI monomer-dimer concentrations	SI8
Figure S10. MecI quantification in MRSA cells	SI8
Figure S11. Western blot of MecI and BlaI proteins	SI8
Figure S12. Plot of MecI binding of <i>mec</i> operator	SI11
Figure S13. Plot of MecI binding of <i>bla</i> operator	SI11

Figure S14. Plot of BlaI binding of <i>mec</i> operator	SI12
Figure S15. Plot of BlaI binding of <i>bla</i> operator.....	SI12
Table S1. Analysis of <i>bla/mec</i> system of <i>S. aureus</i>	SI13
References	SI14

Experimental Procedures

Cloning of the *mecI* gene. Genomic DNA from *S. aureus* NRS70 (N315) was used as the template for cloning. The PCR was performed using the following oligonucleotide primers: *mecI_fw*, 5'-GATATACATATGGATAATAAAACGTATG-3' (*NdeI* restriction site shown underlined) and *mecI_rv3*, 5'-CTCAAGCTTATTTTTTATTCAATATATTTCTCAATTCTTC -3' (*HindIII* restriction site shown underlined). The conditions used for the PCR were as follows: 30 cycles of denaturation at 94 °C for 40 s followed by annealing of primers for 40 s at 60 °C; extension for 1 min at 72 °C using *Pfu* Ultra II DNA polymerase (Stratagene). The reaction volume was 50 µL and contained 10X buffer with 4 mM MgSO₄, 0.2 mM triphosphoryldeoxynucleotides, 0.5 µM of each primer, 50 ng of template DNA, 5% DMSO and 1 µL of *Pfu* Ultra II DNA polymerase. The PCR reaction mixture was subjected to electrophoresis in a 1.5% agarose gel for 25 min at 100 V, and the product was excised and purified using a gel extraction kit (Qiagen). Double digest reaction mixtures using both restriction endonucleases *NdeI* and *HindIII* were carried out on both the PCR product and the empty pET24a(+) vector, and the purified DNA fragments were ligated using T4 DNA ligase (Invitrogen). The ligation mixture was used to transform *Escherichia coli* DH5α (Invitrogen) competent cells. Transformants were selected on LB-agar plates supplemented with 50 µg/mL of kanamycin. To confirm the presence of the inserted *mecI* gene, first we did a colony PCR from several transformants followed by plasmid preparation and digestion with *NdeI* and *HindIII* restriction enzymes. Subsequently, the entire nucleotide sequence of the *mecI* gene was verified by sequencing. The plasmid was designated as pET24-*mecI*.

MecI expression in *E. coli* and purification. We used a modified literature method for this purification.¹ *Escherichia coli* OverExpress C41 (DE3) (Lucigen® Corporation) competent cells were transformed with the pET24-*mecI* plasmid. A colony was selected and cultured overnight in LB media containing 50 µg/mL of kanamycin. This culture was used to inoculate (1/100 dilution) a 1 L culture that was grown to an OD₆₀₀ ~0.8 at 37 °C. At this point protein expression was induced with 0.5 mM IPTG for 4 h at 37 °C. Post-induction cells were harvested by centrifugation for 25 min at 4 °C at 4,000 g and resuspended in 30 mL lysis buffer (50 mM HEPES pH 7.6, 200 mM NaCl, 1 mM EDTA). Then, 1 mM PMSF was added to the resuspended cells, which were subsequently lysed by sonification. The cell debris was removed by centrifugation at 20,000 g at 4 °C for 35 min. The supernatant was loaded onto a 50 mL column with Macro-prep High-Q support (BioRad)

equilibrated in 50 mM HEPES pH 7.6, 200 mM NaCl, 1 mM EDTA and the flow-through was collected and then loaded onto a 50 mL column with Macro-prep High-S support (BioRad) equilibrated in 50 mM HEPES pH 7.6, 200 mM NaCl, 1 mM EDTA. After washing with two column volumes of the same buffer, MecI was eluted using a 240 mL gradient from 0.2-1.0 M NaCl in 50 mM HEPES pH 7.6, 1 mM EDTA. The fractions containing the MecI protein, which eluted at 0.56-0.85 M NaCl, were combined and the NaCl concentration was reduced to 0.2 M by dilution with 50 mM HEPES pH 7.6, 1mM EDTA. The MecI sample was reloaded onto another Macro-prep High-S column (50 mL), washed with two column volumes of 50 mM HEPES pH 7.6, 200 mM NaCl, 1 mM EDTA and eluted with 0.2-1.0 M NaCl gradient. The MecI fractions were pooled and the NaCl concentration was reduced to 0.2 M by dilution with 50 mM Tris pH 7.4. MecI was then passed three times onto a 5 mL Heparin column (GE Healthcare) equilibrated in 50 mM Tris pH 7.4, 0.2 M NaCl with Complete EDTA-free Protease Inhibitor Cocktail (Roche). After washing with five column volumes of the same buffer, the protein was eluted with a 360 mL gradient from 0.2-1.0 M NaCl in 50 mM Tris pH 7.4. MecI eluted at 0.7-0.8 M NaCl. The fractions containing MecI were pooled, the NaCl concentration was decreased to 0.2 M by dilution with 50 mM Tris pH 7.4, and the protein was loaded again onto the Heparin column, but now the protein was eluted using a longer fraction collection. All purification steps were carried out at 4 °C. In each step, the protein content in the column fractions was monitored by SDS-PAGE (Figure S1). The MecI concentration was determined by measuring the absorbance of the solution at 280 nm and using a theoretical extinction coefficient of $26,930 \text{ M}^{-1}\text{cm}^{-1}$. Matrix-assisted laser desorption ionization (MALDI) mass spectrometric analysis revealed a molecular mass of $14,827 \pm 50 \text{ Da}$ for MecI, in agreement with the mass calculated from the gene sequence (14,790 Da) (Figure S2). The homogeneous MecI sample was stored at 4 °C in 50 mM Tris pH 7.4, 0.75 M NaCl. Prior to carrying out equilibrium sedimentation and fluorescence anisotropy assays, the protein was diluted to the desired concentration, followed by one dialysis step against 20 mM MOPS pH 7.4, 200 mM NaCl, 20 mM MgCl_2 and 5% glycerol.

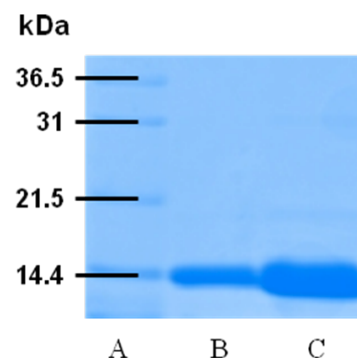


Figure S1. SDS-PAGE analysis of the purified MecI, (A) molecular mass standards, (B) 8 µg MecI and (C) 40 µg MecI

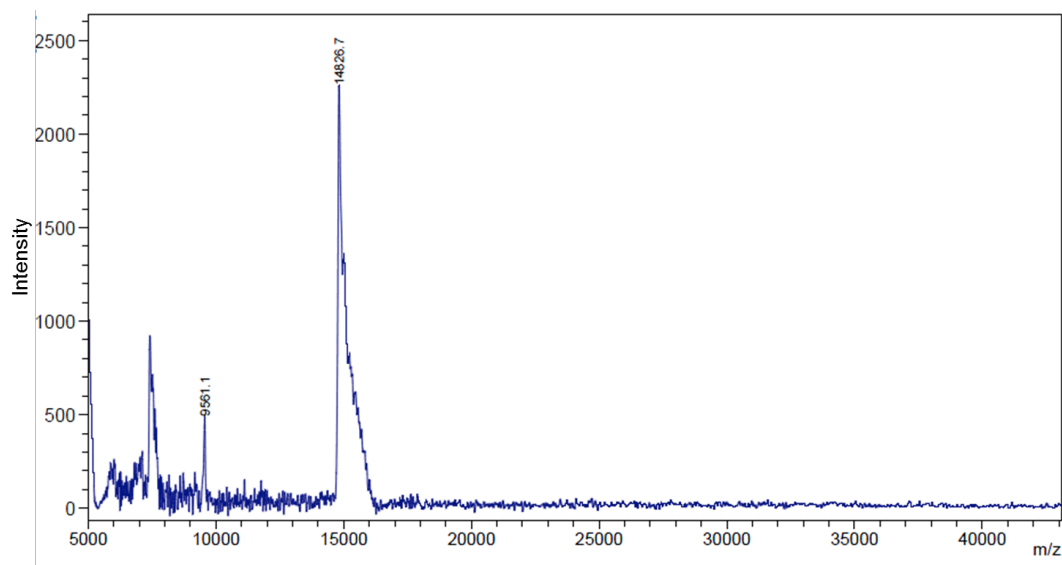


Figure S2. MALDI mass spectrum of 40 µg MecI in 50 mM Tris pH 7.4, 0.75 M NaCl buffer.

Purification of BlaI. BlaI was expressed from the pET-blaI plasmid¹ in *E. coli* OverExpress C41 (DE3), following the same protocol described for the expression and purification of MecI (Figure S3).

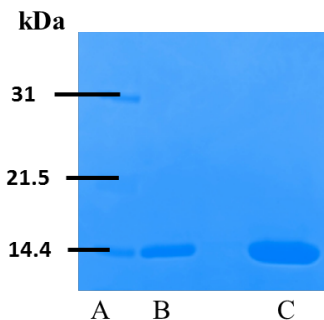


Figure S3. SDS-PAGE analysis of the purified BlaI, (A) molecular mass standards, (B) 5 µg BlaI and (C) 20 µg BlaI

Gel electrophoresis mobility shift assay (EMSA): Two DNA sequences were used. The 41-bp DNA *mec* dsDNA fragment, containing the *mec* operator region, was obtained by annealing a 5' fluorescein-labeled oligonucleotide with an unlabeled reverse complementary oligonucleotide. The HPLC-purified oligonucleotides used in this work were synthesized at Eurofins MWG Operon. The oligonucleotides 5' 6-FAM-ATATAAGACTACATTTGTAGTATATTACAAATGTAGTATTT and 5' AAATACTACATTTGTAATACTACAAATGTAGTCTTATAT were annealed at a 1:1 ratio. Annealing was carried out by heating the reaction mixture to 95 °C for 5 min, followed by slow cooling (overnight) to room temperature in 10 mM Tris pH 7.5. The annealed sample was run on an 18% acrylamide gel in 0.5x Tris-borate-EDTA buffer (TBE), the dsDNA was purified from the gel following the procedure described by Green & Sambrook,² and the concentration was determined from the absorbance at 260 nm. The *bla* dsDNA (*bla* operator), previously designated R1-Z dsDNA, was prepared as described.¹ We combined MecI or BlaI at different concentrations with 0.15 µM *mec* dsDNA or *bla* dsDNA in 20 mM MOPS, 200 mM NaCl, 20 mM

MgCl₂, and 5% glycerol, pH 7.4 and after 45 min of incubation at 22 °C, the resulting mixtures were loaded on an 18% non-denaturing polyacrylamide gel. The gel was subjected to electrophoresis in 0.5X TBE with refrigeration at 70 V for 5 hours (Figure S4). Two protein-DNA complexes could be resolved in the polyacrylamide gel. The same EMSA procedure was followed for BlaI protein with 0.15 μM *mec* dsDNA or *bla* dsDNA (figure S5)

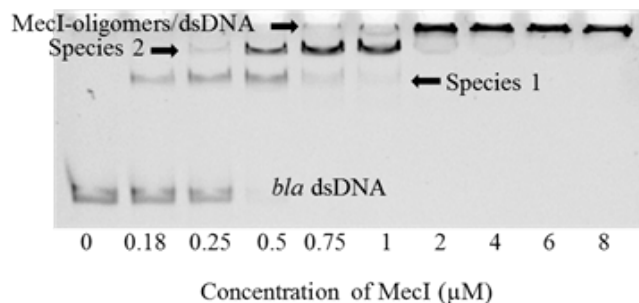


Figure S4. EMSA of MecI binding to *bla* dsDNA.

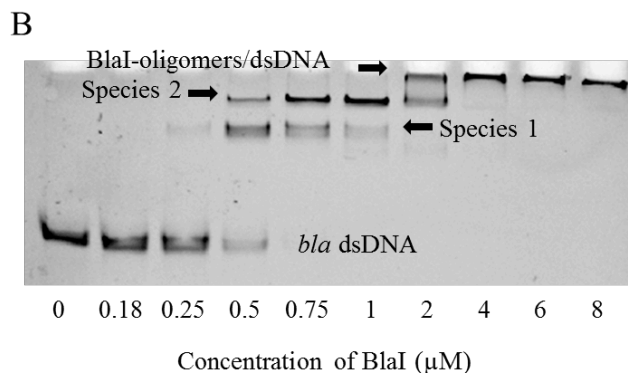
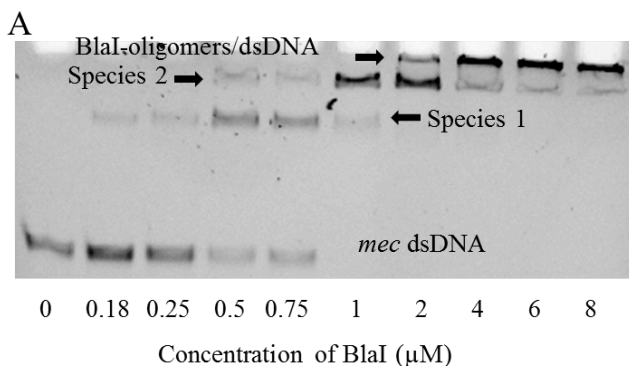


Figure S5. EMSA of BlaI binding to *mec* dsDNA (A) and to *bla* dsDNA (B).

MALDI mass spectroscopy analysis of MecI-dsDNA complexes: We first attempted to characterize the complexes formed at the protein and DNA concentrations used in the EMSA, but the amounts of the different species were too low for detection by MALDI mass spectroscopy. MecI (12 μM) was incubated with 1 μM *mec* dsDNA for 45 minutes at 22°C, and the mixture was subjected to MALDI mass spectroscopy. Under this condition, it was possible to detect two species, which based on their masses (39,188 Da and 54,685 Da) were assigned to the monomer-DNA and dimer-DNA complexes. We also verified by MALDI mass spectroscopy, that MecI forms oligomers at 12 μM; we could detect the monomeric, dimeric, trimeric, tetrameric and pentameric species (Figure 2A).

Sedimentation velocity assay (SV). MecI samples (4-23 μM) in 20 mM MOPS, 200 mM NaCl, 20 mM MgCl_2 , and 5% glycerol, pH 7.4, were loaded (300 μL) into analytical ultracentrifugation cells. The experiments were carried out at 40,000 rpm in a XL-I analytical ultracentrifuge (Beckman-Coulter Inc.) equipped with a UV-VIS absorbance detection system, using an An-50Ti rotor, and 12 mm Epon-charcoal standard double-sector centerpieces. Sedimentation profiles were recorded using the UV-VIS absorbance detection system at 280 nm. Sedimentation coefficient distributions were calculated by least-squares boundary modelling of sedimentation velocity data using the continuous distribution $c(s)$ Lamm equation model as implemented by SEDFIT 14.1.³ These s values were corrected to standard conditions (water, 20 °C, and infinite dilution)⁴ using the program SEDNTERP⁵ to get the corresponding standard s values ($s_{20,w}$). Under these conditions, the MecI sedimentation profile included a main peak at 1.8 S ($s_{20,w} = 2.3\text{S}$) compatible with the protein dimer and a very small fraction of protein (ca 7%) at 1.2 S ($s_{20,w} = 1.6\text{S}$) corresponding to the protein monomer (Figure S6).

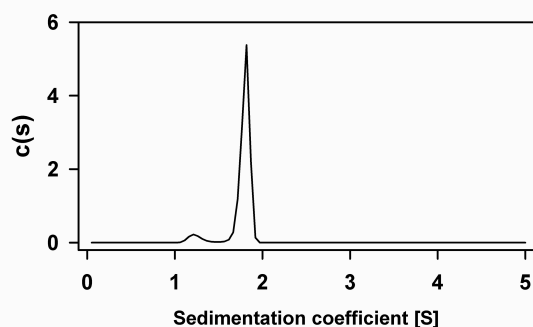


Figure S6. Sedimentation coefficient distribution $c(s)$ profile corresponding to 23 μM purified MecI.

Sedimentation equilibrium assay (SE). Short columns (85 μL) SE experiments of MecI samples (0.5-36 μM) were carried out at speeds ranging from 16,500 to 24,000 rpm and at several wavelengths (229-296 nm), using the same experimental conditions and instrument as in the SV experiments. After the last equilibrium scan, a high-speed centrifugation run (48,000 rpm) was done to estimate the corresponding baseline offsets. Weight-average buoyant molecular weights of protein were determined by fitting a single species model to the experimental data using the HeteroAnalysis program⁶ and corrected for solvent composition and temperature with the program SEDNTERP.⁵ Data collected at different speeds and different loading concentrations were further analyzed globally in terms of different self-association models using SEDPHAT 9.4 software⁷ (Figure S7). Data analysis revealed that MecI exists in solution as a mixture of monomers and dimers at equilibrium with a dissociation constant of $0.30 \pm 0.03 \mu\text{M}$. The observed changes in the average molecular weight evidenced that at high concentration (36 μM) MecI appears mainly as a dimer, Figure S8 shows SE data obtained for MecI at 36 μM and the best-fit analysis assuming the monomer and two different association models. These results were consistent with the SV studies reported above. The program DynaFit⁸ was then used to calculate the concentration of monomer and dimer, and this simulation showed that MecI was present in

solution as both monomer and dimer even at low protein concentrations within the range observed *in vivo* (Figure S9).

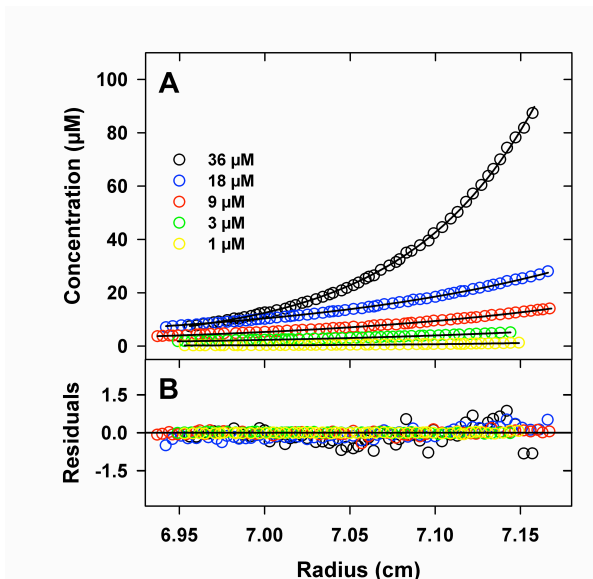


Figure S7. Sedimentation equilibrium analysis of MecI samples. (A) Species distribution from sedimentation equilibrium gradient of MecI (1-36 μM). Open circles and solid lines represent experimental data and best-fit curves of the global analysis to a monomer-dimer model, respectively (B) Distributions of the residuals around a zero mean.

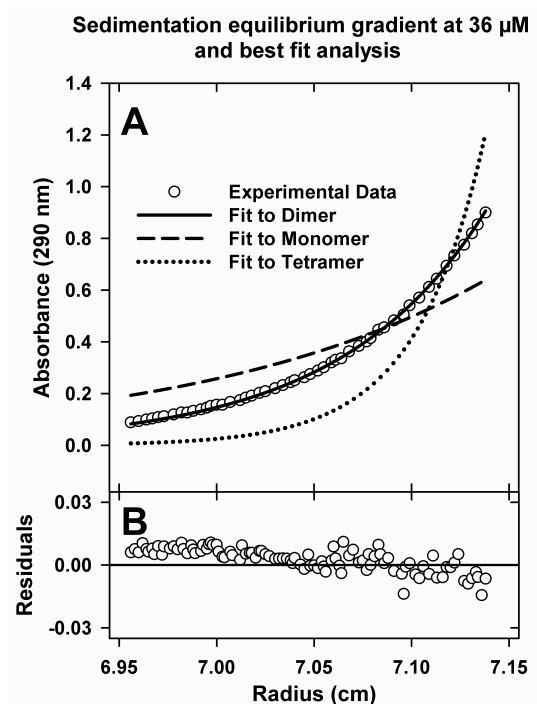


Figure S8. Study of the oligomerization state of MecI protein in solution. (A) Sedimentation equilibrium data (empty circles) and best-fit analysis assuming a protein dimer (black line), monomer (dashed line) and tetramer (dotted line) species. The data indicate that MecI is a dimer at 36 μM . (B) The difference between estimated values and experimental data for protein dimers (residuals).

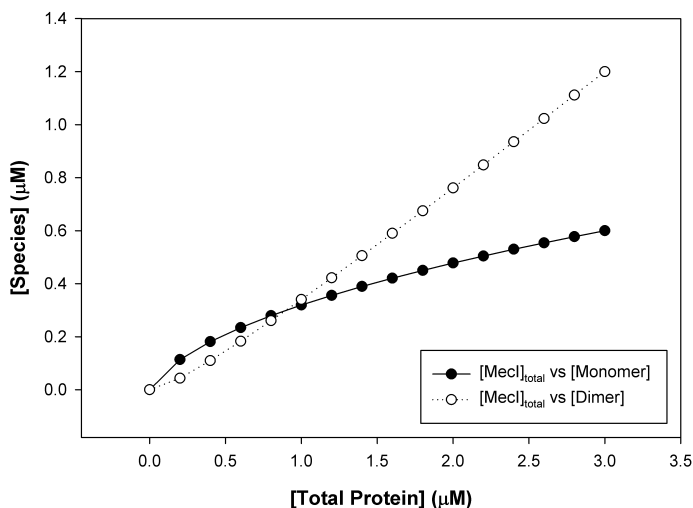


Figure S9. Plot of the calculated concentrations of MecI monomer (closed circles) and of dimer (open circles) against concentration of total protein, based on the equilibrium characterized with a dissociation constant (K_d) of 0.30 ± 0.03 μM . The accumulation of monomer and dimer was evaluated in the range of the *in vivo* concentrations, as determined for *S. aureus* MRSA252.

Determination of the *in vivo* concentration of MecI. The concentrations of MecI in *S. aureus* NRS70 (N315) and MRSA252 strains were determined from cultures grown in the absence of β -lactam antibiotics to exponential and stationary phase, following the procedure previously described.¹ In the case of *S. aureus* MRSA252, as a control to corroborate the identity of the MecI band, oxacillin was added to the cells in the exponential phase (OD_{625} of 0.8) at sub-MIC concentration (0.05 $\mu\text{g}/\text{mL}$), and the culture was then harvested in stationary phase (OD_{625} of 2.3). The MecI bands were quantified using the Image Lab software (BioRad) (Figure S10). Western blotting with purified MecI and BlaI indicated that there was not any cross-reactivity with the anti-MecI antibody (Figure S11).

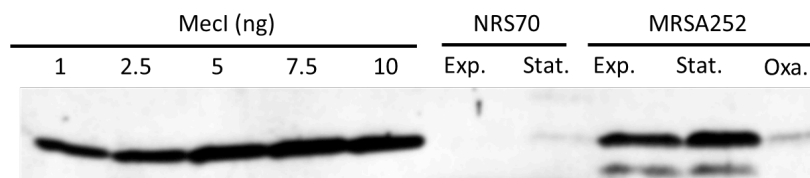


Figure S10. MecI quantification in *S. aureus* cells by Western blot.

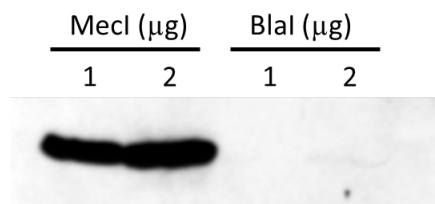


Figure S11. Western blot of MecI and BlaI proteins with anti-MecI antibody.

Characterization of MecI and BlaI binding to *bla* and *mec* operator sequences by fluorescence anisotropy. The dissociation constants for MecI or BlaI binding to the *bla* and *mec* operator regions were determined by the

measurement of the changes in fluorescence anisotropy of fluorescein-labeled dsDNA upon titration with increasing protein concentration. Solutions of MecI or BlaI at different concentrations were prepared in 20 mM MOPS pH 7.4, 200 mM NaCl, 20 mM MgCl₂, 5% glycerol and allowed to equilibrate at room temperature for 1 h. Subsequently, the corresponding fluorescently labeled DNA was added in a final volume of 200 μL to reach a final concentration of 0.1 or 1 nM dsDNA (0.1 nM *bla* dsDNA was used for titration with MecI protein). The samples were mixed and incubated in the dark at room temperature for 1 h. Fluorescence anisotropy measurements were performed on a Beacon 2000 instrument (PanVera, Madison WI) at 25 °C, after 30 s incubation of the mixture in the Beacon equipment. The anisotropy value reported for each sample was the average of two measurements and each complete assay was done in duplicate. The total fluorescence intensity showed no significant change upon addition of different concentrations of protein to the fluorescein-labeled dsDNA samples. The anisotropy values were plotted as a function of total protein concentration and the data were fit in SigmaPlot (Systat Software, San Jose, CA), using different user-defined equations derived to account for seven different models, as described in Llarrull *et al.*¹ The best fit for MecI binding to the *mec* and *bla* operator region was to the model presented in the inset of Figure 3A (Model 1 in Llarrull *et al.*),¹ characterized by the equations detailed below. In the same way, the best fit for BlaI binding to the *mec* operator region was to the same model.

The equations used to fit the DNA-binding data for the model 1 of Llarrull *et al.*¹:

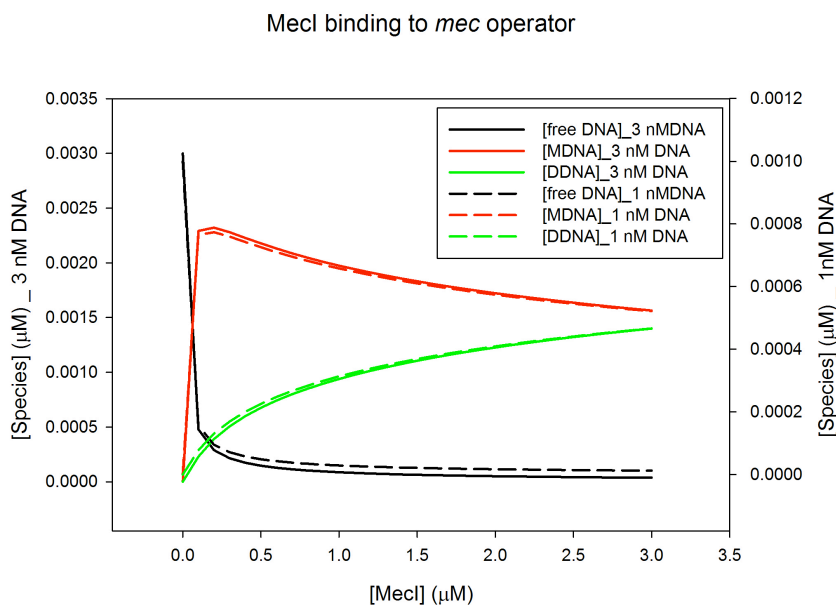
$$A = A_f + \frac{[M]}{K_{d1} \cdot \left(1 + \frac{[M]}{K_{d1}} + \frac{K_d \cdot ([protein]_T - [M])}{2 \cdot K_{d1} \cdot K_{d2}}\right)} \cdot (A_{b1} - A_f) +$$

$$+ \frac{K_d \cdot ([protein]_T - [M])}{2 \cdot K_{d1} \cdot K_{d2} \cdot \left(1 + \frac{[M]}{K_{d1}} + \frac{K_d \cdot ([protein]_T - [M])}{2 \cdot K_{d1} \cdot K_{d2}}\right)} \cdot (A_{b2} - A_f)$$

$$[M] = \frac{-K_d + \sqrt{K_d^2 + 8 \cdot K_d \cdot [protein]_T}}{4}, K_d = \frac{[M]^2}{[D]} \text{ and } K_{d3} = \frac{K_{d1} \cdot K_{d2}}{K_d}$$

Determination of the concentration of protein-bound-DNA and uncomplexed DNA *in vivo*. The *mec* operon is found in a single copy in the chromosome which, given the Avogadro constant (6.022 x 10²³ molecules per 1 mole), gives 1.66 x 10⁻²⁴ moles of *mec* operator DNA per cell. The volume of a *S. aureus* cell is (5.24-14.4) x 10⁻

¹⁶ L, depending on the cell radius (of 500-700 nm).^{9,10} Based on this analysis, the concentration of DNA was calculated as the ratio of the moles of DNA per cell and the cell volume, which gave a concentration of 1-3 nmoles/L of DNA (1-3 nM). The *bla* operon is found either as a single copy in the chromosome (1-3 nM), or as a few copies when present in plasmids (eg. 5 copies in plasmid pI258, which gives a DNA concentration of 5-15 nM). The program DynaFit was used to simulate the concentration of DNA species according to the binding model described in the inset of Fig. 3A, using the dissociation constants derived for each protein-operator pair from the fluorescence anisotropy studies, the dissociation constant that characterizes the dimer-monomer equilibrium for each repressor protein, and the *in vivo* concentration of the repressor proteins. Given the concentration of the *mec* operator *in vivo*, the concentrations of MecI *in vivo*, the MecI dimer-monomer dissociation constant, and the MecI-*mec* dsDNA dissociation constants reported in Table 1, 1-4% of the operator molecules in a *S. aureus* culture would be found uncomplexed and would be available for transcription in the absence of antibiotic (Figure S12). As discussed above, when the concentration of DNA is expressed in nM, we are referring to a volume of 1 L (the volume of a cell is $(5.24-14.4) \times 10^{-16}$ L), which would be equivalent to the volume of $(0.7-1.9) \times 10^{16}$ cells. When we state that 1-4% of the operator molecules in a *S. aureus* culture would be found uncomplexed, it would be equivalent to saying that the genes of the *mec* operon would be transcribed in $0.7-7.6 \times 10^{14}$ cells out of $0.7-1.9 \times 10^{16}$ cells in a liter. A similar scenario is valid for BlaI binding to the *mec* operator region, where 0.7-2.4% of the operator molecules in a *S. aureus* culture would be available for transcription at the *in vivo* BlaI concentrations reported in NRS70 (Figure S13).¹ Binding of BlaI and MecI to the *bla* operator (one or several copies in the cell) *in vivo* would result in higher concentrations of free DNA, and



hence higher levels of transcription in the absence of antibiotic, given the higher values of the dissociation constants for monomer and dimer from the protein-DNA complexes (Figures S14 and S15).

Figure S12. Plot of the calculated concentrations of free DNA and protein-bound forms upon binding of MecI to the *mec* operator, at the *in vivo* concentrations found in *S. aureus* MRSA252.

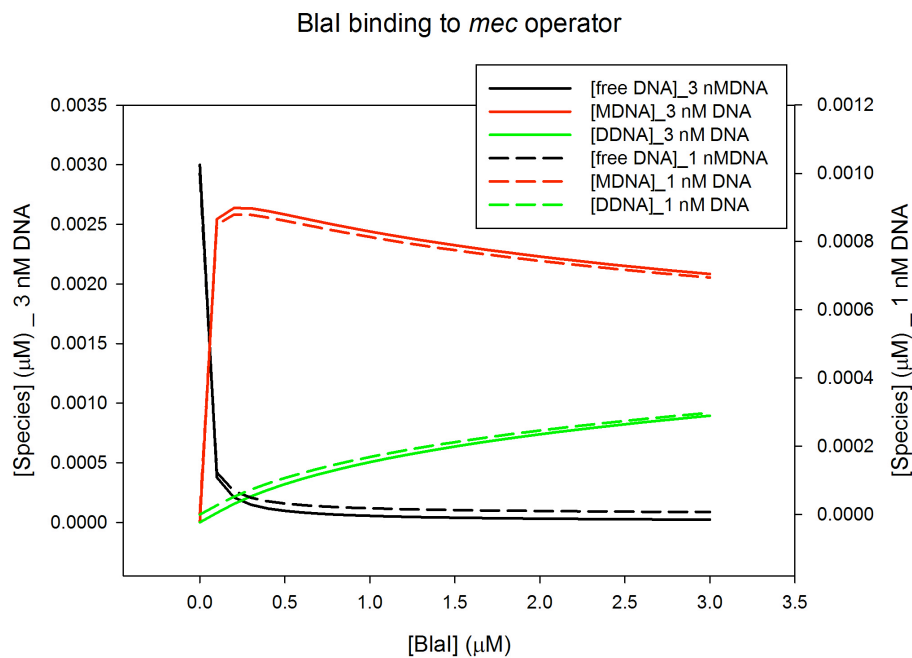


Figure S13. Plot of the calculated concentrations of free DNA and protein-bound forms upon binding of BlalI to the *mec* operator.

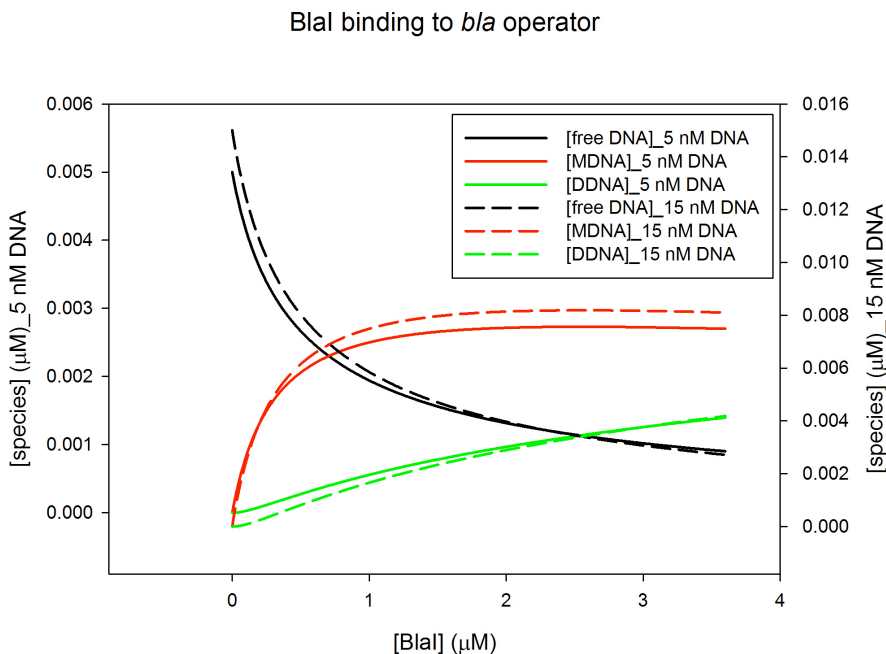


Figure S14. Plot of the calculated concentrations of free DNA and protein-bound forms upon binding of BlalI to the *bla* operator, at the *in vivo* concentrations found in *S. aureus* NRS128.¹

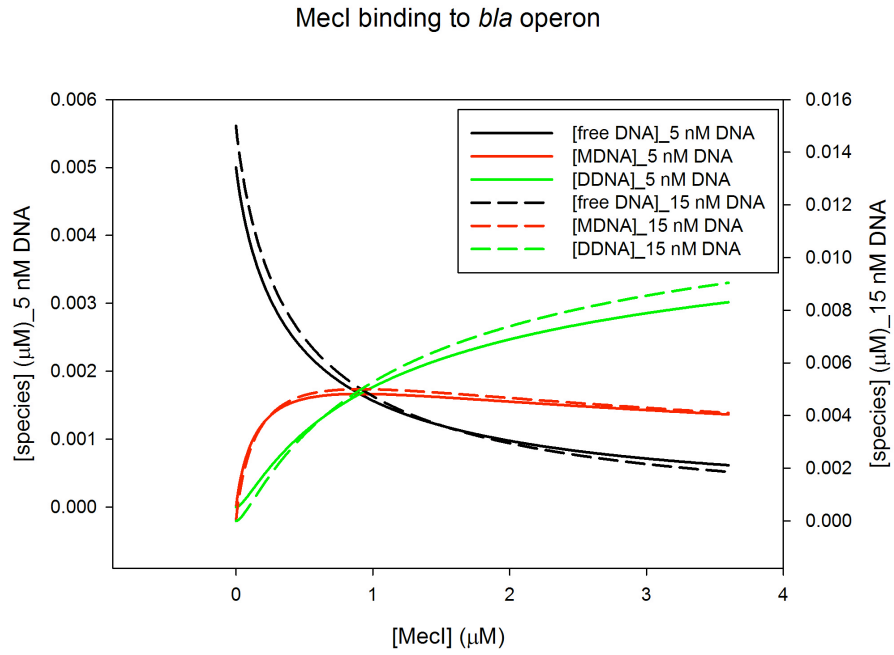


Figure S15. Plot of the calculated concentrations of free DNA and protein-bound forms upon binding of MecI to the *bla* operator.

Table S1. Analysis of the *bla/mec* systems of *S. aureus* genomes deposited at NCBI database^{11,12} (revised by December 2013).

<i>S. aureus</i>		<i>bla</i> system			<i>mec</i> system		
Strain	Taxonomy ID	<i>blaR1</i>	<i>blaI</i>	<i>blaZ</i>	<i>mecR1</i>	<i>mecI</i>	<i>mecA</i>
04-02981	703339	negative	negative	negative	positive	positive	positive
Mu3 (NRS2)	418127	negative	negative	negative	positive	positive	positive
Mu50 (NRS1)	158878	negative	negative	negative	positive	positive	positive
LGA251	985006	negative	negative	negative	positive	positive	positive
N315 (NRS70)	158879	positive	positive	positive	positive	positive	positive
TW20	663951	positive	positive	positive	positive	positive	positive
08BA02176	1229492	positive	positive	positive	positive	positive	positive
CA-347 (USA600) (NRS648)	1323661	positive	positive	positive	positive	positive	positive
JH1	359787	positive	positive	positive	positive	positive	positive
JH9	359786	positive	positive	positive	positive	positive	positive
MRSA252 (NRS71)	282458	positive	positive	positive	positive	positive	positive
JKD6008	546342	positive	positive	positive	positive	positive	positive
Newman	426430	positive	positive	positive	positive	positive	positive
BMB9393	1321369	positive	positive	positive	positive	negative*	positive
Z172	1406863	positive	positive	positive	positive	negative*	positive
T0131	1006543	positive	positive	negative	positive	negative*	positive
COL (NRS100)	93062	negative	negative	negative	negative	negative	positive
M013	1118959	negative	negative	negative	negative	negative	positive
SA957	1201010	negative	negative	negative	negative	negative	positive
USA300_FPR3757	451515	negative	negative	negative	negative	negative	positive
HO 5096 0412	1074252	positive	positive	positive	negative	negative	positive
M1	1305598	positive	positive	positive	negative	negative	positive
11819-97	1123523	positive	positive	positive	negative	negative	positive
CN1	1193576	positive	positive	positive	negative	negative	positive
JKD6159	869816	positive	positive	positive	negative	negative	positive
MSHR1132	985002	positive	positive	positive	negative	negative	positive
MW2 (NRS123)	196620	positive	positive	positive	negative	negative	positive
SA40	1194085	positive	positive	positive	negative	negative	positive
ST398	523796	positive	positive	positive	negative	negative	positive
TCH60	548473	positive	positive	positive	negative	negative	positive
USA300 TCH1516	451516	positive	positive	positive	negative	negative	positive
NRS128	na	positive	positive	positive	negative	negative	negative
55/2053	585143	positive	positive	positive	negative	negative	negative
6850	1392476	positive	positive	positive	negative	negative	negative
ECT-R 2	889933	positive	positive	positive	negative	negative	negative
MSSA476	282459	positive	positive	positive	negative	negative	negative
71193	1155084	positive	positive	negative	negative	negative	negative
VC40	1028799	negative	negative	negative	negative	negative	negative
RF122	273036	negative	negative	negative	negative	negative	negative
ED98	681288	negative	negative	negative	negative	negative	negative
ED133	685039	negative	negative	negative	negative	negative	negative

na means not available.

positive indicates presence of the gene in the genome.

negative indicates absence of the gene in the genome.

* Strain that carries a *mecI* gene with a mutation that introduces a stop codon.

REFERENCES

1. Llarrull, L. I., Prorok, M., Mobashery, S. (2010) Binding of the gene repressor to the *bla* operon in Methicillin Resistant *Staphylococcus aureus*, *Biochemistry* 49, 7975-7977.
2. Green, M. R., Sambrook, J. (2012) Molecular cloning: A laboratory manual. *Cold Spring Harbor Laboratory Press*.
3. Schuck, P. (2000) Size-distribution analysis of macromolecules by sedimentation velocity ultracentrifugation and lamm equation modeling. *Biophys. J.* 78, 1606-1619.
4. van Holde K. E. (1985) Physical Biochemistry. 2nd Ed., *Prentice-Hall, Englewood Cliffs, N.*
5. Laue, T. M., Shah, B. D., Ridgeway, T. M., Pelletier, S. L. (1992) Computer-aided interpretation of analytical sedimentation data for proteins, *Anal. Ultracentrifugation Biochem. Polym. Sci.* 90-125.
6. Cole, J. L. (2004) Analysis of heterogeneous interactions, *Methods Enzymol.* 384, 212-232.
7. Vistica, J., Dam, J., Balbo, A., Yikilmaz, E., Mariuzza, R. A., Rouault, T. A., Schuck, P. (2004) Sedimentation equilibrium analysis of protein interactions with global implicit mass conservation constraints and systematic noise decomposition. *Anal. Biochem.* 326, 234-256.
8. Kuzmic, P. (1996) Program DYNAFIT for the Analysis of Enzyme Kinetic Data: Application to HIV Proteinase, *Anal. Biochem.* 237, 260-273.
9. Wyatt, P. J. (1970) Cell wall thickness, size distribution, refractive index ratio and dry weight content of living bacteria (*Staphylococcus aureus*), *Nature* 226, 277-279.
10. Beltramini, A. M., Mukhopadhyay, C. D., Pancholi, V. (2009) Modulation of cell wall structure and antimicrobial susceptibility by a *Staphylococcus aureus* eukaryote-like serine/threonine kinase and phosphatase, *Infect. Immun.* 77, 1406-1416.
11. Sayers, E. W., Barrett, T., Benson, D. A., Bryant, S. H., Canese, K., Chetvernin, V., Church, D. M., DiCuccio, M., Edgar, R., Federhen, S., Feolo, M., Geer, L. Y., Helmberg, W., Kapustin, Y., Landsman, D., Lipman, D. J., Madden, T. L., Maglott, D. R., Miller, V., Mizrachi, I., Ostell, J., Pruitt, K. D., Schuler, G. D., Sequeira, E., Sherry, S. T., Shumway, M., Sirotkin, K., Souvorov, A., Starchenko, G., Tatusova, T. A., Wagner, L., Yaschenko, E., Ye, J. (2009) Database resources of the National Center for Biotechnology Information, *Nucleic Acids Res.* 37, 5-15.
12. Benson, D. A., Karsch-Mizrachi, I., Lipman, D. J., Ostell, J., Sayers, E. W. (2009) GenBank, *Nucleic Acids Res.* 37, 26-31.